ChemComm

Supramolecular Traps for Highly Phosphorylated Inositol Sources of Phosphorus

Journal:	*ChemComm*
Manuscript ID	CC-COM-11-2019-009321.R1
Article Type:	Communication

COMMUNICATION

Supramolecular Traps for Highly Phosphorylated Inositol Sources of Phosphorus

Received 00th January 20xx,
Accepted 00th January 20xx

DOI: 10.1039/x0xx00000x

Subhamay Pramanik,[a] Victor W. Day [a] and Kristin Bowman-James*[a]

Structurally elusive inositol hexakisphosphates have been trapped in host-guest sandwiches between two picolinamide macrocycles that remain intact in solution, aided by hydrogen bonds and electrostatic interactions. This first report of macrocyclic complexes of inositol hexakisphosphates provides structural insight to significant biosources of phosphorus that impact the global phosphorus cycle.

Global concern over depleting phosphorus reserves has intensified the research on phosphorus and phosphorus-containing species, such as phosphates and organophosphates. Furthermore, inositol phosphates have been cited as a major knowledge gap in understanding the global phosphorus cycle.[1] The inositol-1,2,3,4,5,6-hexakisphosphates (IP_6) are especially under scrutiny due to the large number of phosphates contained in these relatively small ions. The *myo* stereoisomer of IP_6 and the most abundant of the nine stereoisomers, has been given the name phytate. It is found in all eukaryotes and is prevalent in plant tissues, pollen, seeds, nuts, and legumes[2,3] (Fig. 1A). Phytate has numerous metabolic roles including in signal transduction, cell regulation, and storage and retrieval of phosphorus. Together, with phosphorylated breakdown products, inositol phosphates are frequently the most abundant of the organophosphates found in soils,[2] in some soils rivalling that of inorganic phosphates.[4] More recently phytate has become increasingly recognized for applications-oriented uses, such as in providing the crosslinking networks for the formation of strong hydrogels[5] and in acid stable metal-organic frameworks.[6]

Under *in vivo* conditions, the myo stereoisomer, phytate, is generally multiply-charged and acts as a metal ion magnet, resulting in insoluble deposits of metal salts. The ensuing loss of bioavailability of important mineral nutrients such as calcium, iron and zinc, has led to phytate being classified as an antinutrient in soils and aquatic ecosystems. Of these, *scyllo*-IP_6 is the next most abundant stereoisomer (Fig. 1B). *Scyllo*-IP_6 is not found in plants, although non-phosphorylated *scyllo*-inositol is found in biosystems.[7] Despite some knowledge of the roles of the non-phosphorylated *scyllo*-inositol, including in neurodegenerative diseases such as Alzheimers, there is little known about possible roles that *scyllo*-IP_6, or indeed the other stereoisomers, might play *in vivo*.

The chemical complexity of the nine possible stereoisomers of the inositol hexaphosphates is amplified by the large number of phosphate groups on the individual inositols. These species can range from neutral ($H_{12}IP_6$) to a highly charged (IP_6^{12-}) depending on pH. Within the scope of this discussion, IP_6 without charges and/or hydrogen atoms will refer to inositol hexakisphosphates in general. The term phytate is reserved only for the *myo* isomer. Phytate has two main chair conformations, the 1a5e, found at lower pHs, and the 5a1e, usually occurring at pHs above nine or ten (Fig. 1A). A similar chair conformation change is observed for *scyllo*-IP_6, from 6e at low pH to 6a at high pHs (Fig. 1B). The pHs at which these conformation changes occur are dependent on other solution influences, including counterion charge.[8]

The inositol phosphates have presented major challenges to a wide range of scientists across agricultural, biological, chemical, geochemical, and environmental fields. Clearly, a better understanding of the structures of inositol phosphates in different environments can help to address some of these challenges. However, crystal structures for even simple metal ion phytate salts have been elusive due to the uncanny aptitude of phytate for forming amorphous solids. Structures of only three metal ion salts of phytate have been reported to date, Na^+, Zn^{2+}, and K^+.[9,6,10] More recently Kremer and Bianchi published a series of papers of both simple protonated o-phenanthroline and terpyridine host-guest complexes of phytate, as well as phytate transition metal complexes of Cu(II) and Mn(III) with these chelating ligands. Their studies have helped pave the way for a better understanding of the structural aspects of phytate.[11-14]

[a] *Department of Chemistry, University of Kansas, Lawrence, Kansas 66045, USA. Email: kbjames@ku.edu*

† Electronic Supplementary Information (ESI) available: For Materials, Instrumentation, synthetic procedures, spectroscopic analysis and X-ray crystallographic studies (CCDC 1947224, 1947225, 1947283). See DOI: 10.1039/x0xx00000x

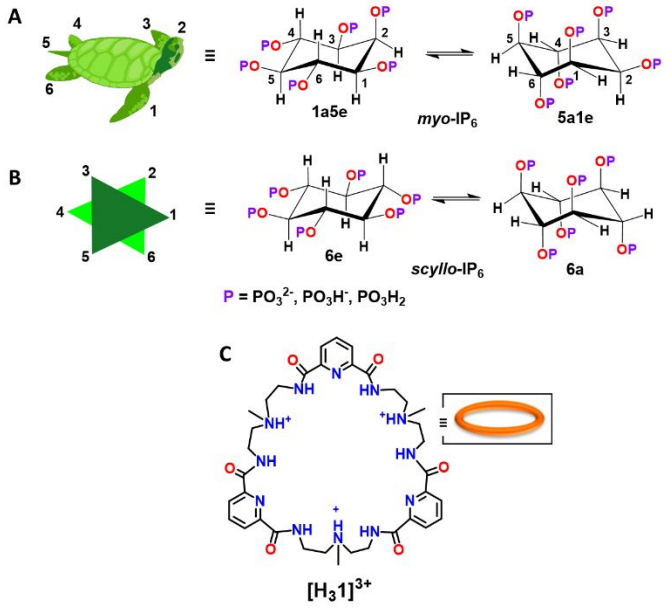

Fig. 1 The chemical players - $H_6IP_6^{6-}$ guests and macrocyclic host: (A) cartoon showing the *myo*-IP_6 turtle and ChemDraw schematic of its 1a5e ↔ 5a1e conformation flip; (B) cartoon showing the *scyllo*-IP_6 hexagon and ChemDraw schematic of its 6e ↔ 6a conformation flip; and (C) ChemDraw diagram of the triprotonated macrocyclic host [H_3**1**$^{3+}$].

Given our earlier experience in using synthetic macrocyclic hosts for binding nucleotides,[15-18] we decided to tackle the crystallographic challenge of trapping phytate using macrocyclic cages. Here we report binding and crystallographic results for the first supramolecular *macrocyclic* complexes of two inositol hexakisphosphates, including the first crystallographic report of the *scyllo* isomer. The relatively large 36-membered ring macrocycle forms sandwich traps of single anions of both *myo*- and *scyllo*-$H_6IP_6^{6-}$ stereoisomers, separated into crystals of two different morphologies. Together with the solution structural and binding studies, these findings provide additional insight to intra- and inter-ionic interactions of these structurally elusive stereoisomers of IP_6.

To aid in identifying conformations, the phosphate positions for phytate in the 1a5e conformation have been compared to the structure of a turtle, known as Agranoff's turtle[19] (Fig. 1A). The upturned head is assigned to the axial P2, the tail to the equatorial P5, and the legs to the other four phosphates. To our knowledge, the conformation of the *scyllo*-IP_6 has not been assigned to any animal species. Thus, we propose portraying it as a compressed trigonal antiprism due to the slightly up-down alternating orientations of the equatorial phosphates (Fig. 1B).

The macrocycle **1** can be obtained via stepwise condensations between dimethyl-2,6-pyridinedicarboxylates and N-methyl-2,2'-diaminodiethylamines (Scheme S1 and Figs. S1-S12, ESI†), and contains three pyridine-2,6-dicarboxamide and three tertiary amine groups (Fig. 1C and Figs. S18 and S19, ESI†). Preliminary NMR studies of the commercially available dipotassium phytate salt, $[K]_2[H_{10}IP_6]$, with **1** indicated a significant affinity of the phytate for the 36-membered ring macrocycle. The *scyllo* isomer was only a minor contaminant of the phytate reagent, yet amazingly it was cleanly separated from the bulk phytate ions by the macrocyclic crystallization.

The two stereoisomers crystallized with different morphologies from the same H_2O:MeOH:DMSO:CH_3CN solution (2:2:1:1, pH 6.26, RT). The solution was obtained by adding $[K]_2[H_{10}IP_6]$ dissolved in H_2O into a CH_3OH solution of the macrocycle, **1**. DMSO and CH_3CN were added to achieve a clear solution and the crystals grew over a several month period. Thin platelet crystals containing the *myo* isomer were found to belong to the monoclinic space group *C2/c*, and rhombohedral crystals of the *scyllo* complex crystallized in the $R\bar{3}$ space group (Fig. 2A) to give $[(H_3\mathbf{1}^{3+})_2(myo\text{-}H_6IP_6^{6-})]\cdot 36.6H_2O\cdot CH_3OH$ (Fig. 2B and Fig. S20, ESI†) and $[(H_3\mathbf{1}^{3+})_2(scyllo\text{-}H_6IP_6^{6-})]\cdot 25.7H_2O\cdot 2CH_3CN$ (Fig. 2D and Fig. S21, ESI†), respectively (Table S2, ESI†).

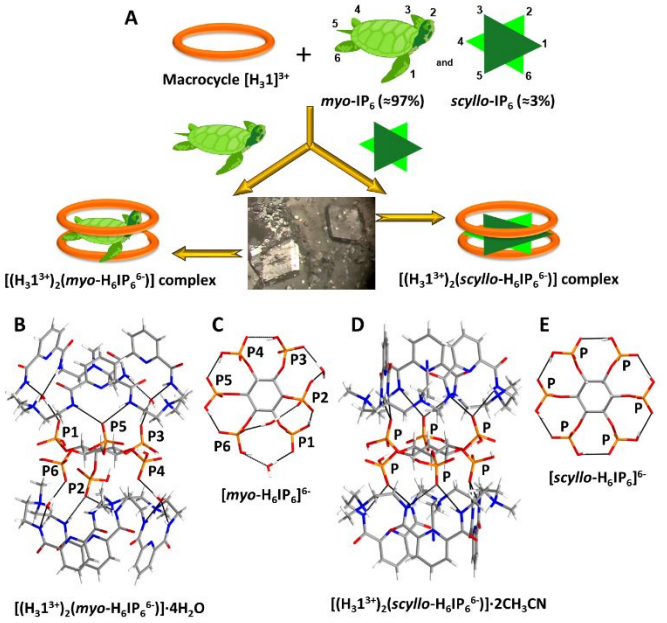

Fig. 2 (A) Stereoisomer separation scheme and photograph of the *myo*- and *scyllo*-crystal forms; perspective views of (B) the *myo*-$H_6IP_6^{6-}$ sandwich complex; (C) an isolated *myo*-$H_6IP_6^{6-}$ ion; (D) the *scyllo*-$H_6IP_6^{6-}$ complex; and (E) an isolated *scyllo*-$H_6IP_6^{6-}$ ion. Only H_2O molecules relevant to the IP_6^{6-} binding are shown.

Isolation of the rhombohedral *scyllo* crystals enabled the first crystal structure of the *scyllo*-IP_6 conformer. Spectra of the integrated ^{1}H NMR signals indicated that only about 3% of the *scyllo*-stereoisomer was present (Figs. S13-S14, ESI†). Kremer and Bianchi had also observed a minor component of the *scyllo*-IP_6 in a disordered phytate in one of their supramolecular terpyridine complexes,[11] but this is the first crystallographic report of a *scyllo*-IP_6 salt.

In both the *myo*- and *scyllo*-$H_6IP_6^{6-}$ structures the macrocycles are folded with the pyridine groups pointing away from the sandwiched $H_6IP_6^{6-}$ ions, leaving the more hydrophilic amide NH groups pointed toward the anion. All six phosphates are monoprotonated in both stereoisomers, and alternating P=O groups point either upward or downward toward the macrocycles (Figs. 2B and D), while the negatively charged phosphates form intramolecular chelate rings around the "equator" of the $H_6IP_6^{6-}$ ions (Figs. 2C and E). However, only two direct hydrogen bond interactions from P2=O and P5=O were observed between the *myo*-$H_6IP_6^{6-}$ anion and the macrocycle

dicarboxamide chelate groups (NH···O=P = 2.83(9) to 3.01(9) Å). Oxygen atoms on the other four P=O groups (P1, P3, P4, and P6) interact with the upper and lower macrocycles through bridging H_2O molecules (Fig. 2B). The phosphates in the *myo*-$H_6IP_6^{6-}$ anion form strong, direct intramolecular hydrogen bonds with neighbouring phosphate oxygen atoms ranging from 2.53(8) to 2.58(5) Å (Fig. 2C), except for P2 and P3, and P1 and P6, which are chelated to each other through bridging H_2O molecules. In addition to its direct interaction with the macrocyclic amide NH groups, the axial P2=O, bridges to P6=O through a H_2O molecule.

While there are clear similarities to the two structures as noted above, the inherent symmetry of the 6e conformation in the *scyllo*-isomer carries over to its S_6 symmetrical crystal structure. Alternating neutral P=O phosphate groups are chelated directly to macrocyclic dicarboxamide chelates through NH···O=P interactions (NH···O=P = 2.90(1) and 2.99(1) Å). Unlike in the *myo* structure, there is a very symmetrical, girdle of direct hydrogen-bond P-OH···(-)O-P linkages around the *scyllo*-$H_6IP_6^{6-}$ equator. These interactions are longer than those in the myo isomer (2.83(2) Å compared to an average of 2.56(8) Å in the *myo*-$H_6IP_6^{6-}$) (Fig. 2D). Also, unlike the *myo* structure, in the *scyllo* sandwich an acetonitrile molecule is encapsulated within each of the pyridine "crowns." The cyanide C≡N groups point outward (methyl groups toward the *scyllo*-IP_6), and the distance between the ring centre of gravity and the midpoint of the C≡N bond is 3.62 Å, potentially indicating some π-π interactions between the acetonitrile and the pyridines.

A key feature of both structures is that the macrocycle has succeeded in isolating single $H_6IP_6^{6-}$ ions from each other in the solid state. As seen in the crystal packing, viewed minus the large water component, distances between the $H_6IP_6^{6-}$ anions range from 9.44 to 11.23 Å (P4---P4 and P1---P1, respectively) for the *myo* structure (Fig. 3A), and are 11.52 Å (P---P) for the *scyllo* stereoisomer (Fig. 3B). However, if the fraction of H_2O molecules inhabiting the region between the two complexes is included, the H_2O clearly provides buffer zones around adjacent complexes (Figs. 3C and D). Both DOSY studies and NMR titrations indicate that the sandwiches remain intact in solution, which is an indication of the strength of this H_2O solvation shell.

^{1}H NMR studies were performed to determine if the sandwich complexes remained intact in solution. Given that the number of *scyllo* crystals was limited, the experimental NMR results are primarily for the *myo*-IP_6, phytate. Since the phytate reagent, $[K^+]_2[H_{10}IP_6^{2-}]$, is only soluble in H_2O and sparingly soluble in DMSO, and **1** is soluble in DMSO or a DMSO-H_2O mixture, DMSO-d_6:D_2O (1:1) was chosen as the solvent system for the solution studies. The apparent pH of a 1:1 DMSO-d_6:D_2O mixture is slightly higher than that of pure D_2O (8.16 in 1:1 DMSO-d_6:D_2O compared to 7.37 in D_2O). The pHs noted here are not corrected for this difference.

The neutral macrocycle (**1**) was dissolved in a DMSO-d_6:D_2O (1:1) solution (pH = 8.12) and titrated with a DMSO-d_6:D_2O solution of $[K^+]_2[H_{10}IP_6^{2-}]$ (pH = 3.51). Upon adding phytate, the amide NH signals shifted downfield, as well as the methylene (H_a, H_b) and methyl (H_c) protons (Figs. 4A and B). After addition of one equivalent of phytate to two equivalents of **1**, saturation of the amide shift was observed (Δδ = 0.77 ppm). Upon further addition of phytate, no significant change was noted, and the signal sharpened, indicating a 2:1 macrocycle:phytate sandwich complex. These results were accompanied by a lowering of pH to 5.87 as anticipated by the addition of the acidic phytate solution. Binding constants of **1** with $[K^+]_2[H_{10}IP_6^{2-}]$ indicated a strong affinity of the phytate for a second macrocycle, $K_{1:1}$ = 3.35 x 10^3 M^{-1} and $K_{2:1}$ > > 10^5 M^{-1} using EQNMR.[20] Binding to the second macrocycle was beyond the normal NMR limits. The "reverse" ^{31}P NMR titration of the chemical shifts of the phytate phosphorus signals on addition of the macrocycle **1** also indicates 1:2 binding of phytate with macrocycle **1** (Figs. 4C and D). Solution studies are further supported by ESI-MS of redissolved phytate crystals, with peaks corresponding to 2:1 sandwich complex formation (Fig. S15, ESI†).

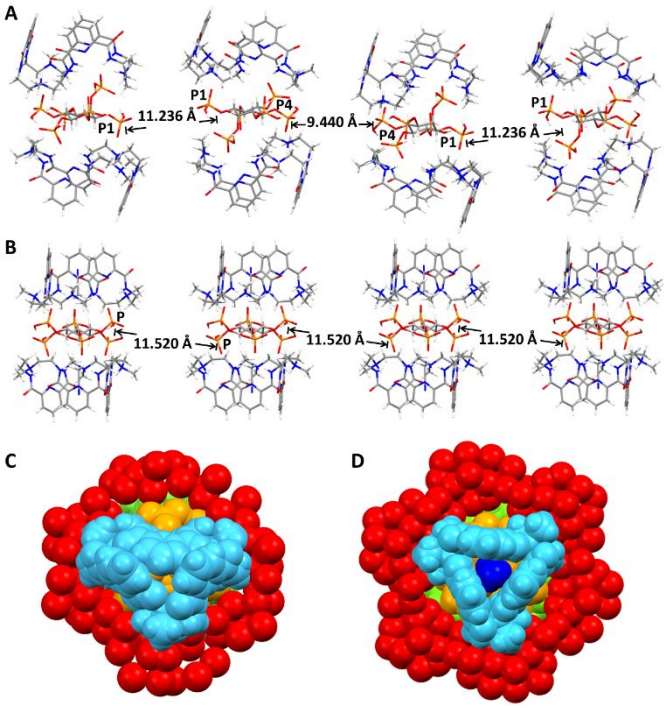

Fig. 3 Packing and overhead views: Packing diagrams without waters viewed down the *b* axes for (A) $[(H_3\mathbf{1}^{3+})_2(myo\text{-}H_6IP_6^{6-})]$ and (B) $[(H_3\mathbf{1}^{3+})_2(scyllo\text{-}H_6IP_6^{6-})]$; and overhead space-filling views of single complexes surrounded by H_2O buffer layers for (C) $[(H_3\mathbf{1}^{3+})_2(myo\text{-}H_6IP_6^{6-})]$ and (D) $[(H_3\mathbf{1}^{3+})_2(scyllo\text{-}H_6IP_6^{6-})]$ surrounded by H_2O buffer layers. Color schemes for (C) and (D) are light blue (top macrocycle), light green (bottom macrocycle), yellow-orange (phytate), red (H_2O oxygen atoms), and dark blue for the acetonitrile in the *scyllo* structure in (D).

Diffusion ordered spectroscopy (DOSY) was used for determining the molecular size of the species in solution. Diffusion coefficients (*D*) were obtained using the NMR titration sample at the 2:1 saturation point. The hydrodynamic radius (r_s) was calculated using the Stokes-Einstein equation (Fig. 5, Table S1 and Figs. S16-S17, ESI†). The crystal structures of the free base **1** and the $[(H_3\mathbf{1}^{3+})_2(myo\text{-}H_6IP_6^{6-})]$ complex were used to determine their sizes (Fig. S18 and S22, ESI†).

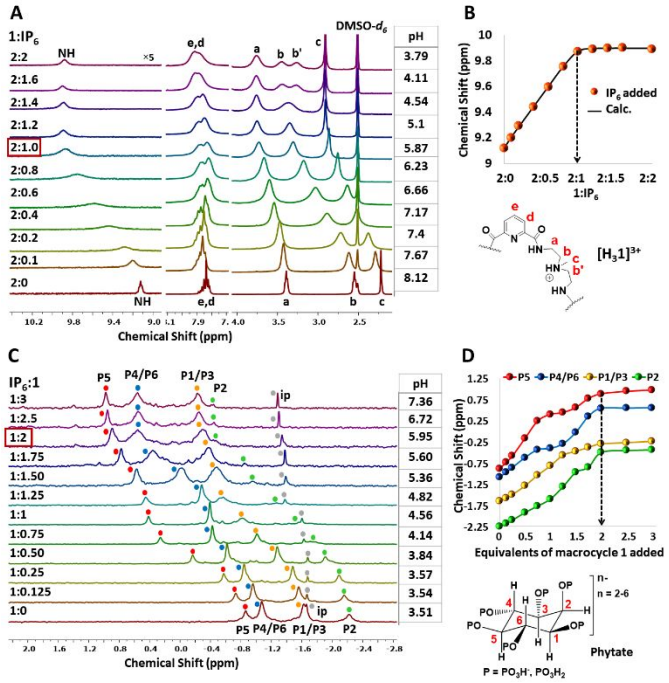

Fig. 4 NMR titration studies of macrocycle **1** and phytate. (A) ^{1}H chemical shift changes on addition of phytate to **1**. (B) Binding curve of the amide NH protons of **1** as a function of added aliquots of phytate. (C) ^{31}P chemical shift changes on addition of **1** to phytate. (D) Binding curves of the phytate ^{31}P signals as a function of added aliquots of **1**. All studies were performed in DMSO-d_6:D_2O (1:1).

The diameter ($2r_s$) for the solution species containing the macrocycle **1** and phytate was found to be 21.72 Å. This distance compares well with the crystallographic length observed for $[(H_3\mathbf{1}^{3+})_2(myo\text{-}H_6IP_6^{6-})]$ of 22.30 Å, measured between the uppermost point in the upper macrocycle to the lowest point in the lower macrocycle (Fig. 5 and Table 1). Sizes of the different components, including the free base of **1**, the complex, and the phytate in the complex (Fig. S18 and S22, ESI†) agree well with the DOSY calculations, as well as with the phytate size from our recently reported $[(K^+)_3(myo\text{-}IP_6^{3-})]$[10] salt (Table S1, ESI†). These results indicate that the sandwiched phytate complex holds together in solution.

Table 1. Comparison of DOSY-determined diameters with crystallographic diameters.

Samples	D (×10^{-6} cm^{2}s^{-1})[1]	DOSY Diameter (Å)	Crystal Diameter (Å)
myo-IP_6^{n-} (1a5e)	4.05	9.8	10.3
1	1.01	15.3	16.0
$[(H_3\mathbf{1}^{3+})_2(myo\text{-}H_6IP_6^{6-})]$	0.71	21.7	22.3

[1]D is the diffusion coefficient.

To summarize, supramolecular host-guest chemistry involving hydrogen bond and electrostatic interactions has enabled trapping and separation of two structurally elusive, hexaphosphorylated inositol ions. These structures represent two of only a handful of structures of *myo*-IP_6 and the first structure of a *scyllo*-IP_6 ion. The large macrocyclic hosts shield isolated IP_6^{6-} ions from the surrounding bulk water, which, in turn, forms buffer zones around each macrocyclic complex. Additional ^{1}H and ^{31}P NMR titrations and DOSY solution studies indicate that the complexes also remain intact in solution, possibly attributed to the strong complexation between the hosts and guests and the H_2O buffer zones. The outlook is bright for macrocyclic and other supramolecular hosts to serve as biomimetic traps for complex biomolecules such as the inositol phosphates.

The authors thank the National Science Foundation (CHE-1710535) for support of this work and (CHE-0923449) for the purchase of the X-ray diffractometer. The authors thank Dr. Justin T. Douglas, Director of the NMR Laboratory at the University of Kansas, for helpful NMR discussions.

Conflicts of interest

There are no conflicts to declare.

Notes and references

1 B. L. Turner, M. J. Papházy, P. M. Haygarth and I. D. McKelvie, *Phil. Trans. R. Soc. Lond. B*, 2002, **357**, 449.
2 V. Raboy, *Plant Sci.*, 2009, **177**, 281.
3 V. Raboy, *Phytochemistry*, 2003, **64**, 1033.
4 H. Whitfield, A. M. Riley, S. Diogenous, H. Y. Godage, B. V. L. Potter and C. A. Brearley, *Plant Soil*, 2018, **427**, 149.
5 L. Xu, C. Wang, Y. Cui, A. Li, Y. Qiao and D. Qiu, *Sci Adv.*, 2019, **5**, eaau3442.
6 K. Cai, F. Sun, X. Liang, C. Liu, N. Zhao, X. Zou and G. Zhu, *J. Mater. Chem. A*, 2017, **5**, 12943.
7 M. P. Thomas, S. J. Mills and B. V. L. Potter, *Angew. Chem. Int. Ed.*, 2016, **55**, 1614.
8 N. Veiga, J. Torres, I. Macho, K. Gómez, G. González and C. Kremer, *Dalton Trans.*, 2014, **43**, 16238.
9 G. E. Blank, J. Pletcher and M. Sax, *Biochem. Biophys. Res. Commun.*, 1971, **44**, 319.
10 M. Reinmuth, S. Pramanik, J. T. Douglas, V. W. Day and K. Bowman-James, *Eur. J. Inorg. Chem.*, 2019, **2019**, 1870.
11 N. Veiga, J. Torres, C. Bazzicalupi, A. Bianchi and C. Kremer, *Chem. Commun.*, 2014, **50**, 14971.
12 D. Quiñone, N. Veiga, J. Torres, J. Castiglioni, C. Bazzicalupi, A. Bianchi and C. Kremer, *Dalton Trans.*, 2016, **45**, 12156.
13 D. Quiñone, N. Veiga, J. Torres, J. Castiglioni, C. Bazzicalupi, A. Bianchi and C. Kremer, *ChemPlusChem*, 2017, **82**, 721.
14 D. Quiñone, S. Martínez, F. Bozoglián, C. Bazzicalupi, J. Torres, N.Veiga, A. Bianchi and C. Kremer, *ChemPlusChem*, 2019, **84**, 540.
15 P. G. Yohannes, M. P. Mertes and K. B. Mertes, *J. Am. Chem. Soc.*, 1985, **107**, 8288.
16 M. P. Mertes and K. B. Mertes, *Acc. Chem. Res.*, 1990, **23**, 413.
17 L. Qian, Z. Sun, J. Gao, B. Movassagh, L. Morales and K. B. Mertes, *J. Coord. Chem.*, 1991, **23**, 155.
18 A. Bencini, A. Bianchi, E. García-España, E. C. Scott, L. Morales, B. Wang, M. P. Mertes and K. B. Mertes, *Bioorg. Chem.*, 1992, **20**, 8.
19 B. W. Agranoff, *Trends Biochem. Sci.*, 1978, **3**, N283.
20 M. Hynes, *J. Chem. Soc., Dalton Trans.*, 1993, **2**, 311.

Table of contents entry

Polyamide macrocycle enables crystallization and separation of two stereoisomers of inositol-1,2,3,4,5,6-hexakisphosphate, providing structural insight to a significant biosource of phosphorus.